

Interactional effects of bubble size, particle size, and collector dosage on bubble loading in column flotation

A. Eskanlou¹, M.R. Khalesi^{1*}, M. Abdollahy¹ and M. Hemmati Chegeni²

1. Department of Mining Engineering, Faculty of Engineering & Technology, Tarbiat Modares University, Tehran, Iran
2. Mining Engineering Department, Arak University of Technology, Arak, Iran

Received 29 May 2017; received in revised form 13 July 2017; accepted 16 July 2017

*Corresponding author: mrkhalesi@modares.ac.ir (M.R. Khalesi).

Abstract

The success of flotation operation depends upon the thriving interactions of chemical and physical variables. In this work, the effects of particle size, bubble size, and collector dosage on the bubble loading in a continuous flotation column were investigated. In other words, this work was mainly concerned with the evaluation of the true flotation response to the changes in the operating variables in column flotation. Two bubble sizes of 0.8 and 1.8 mm, three size fractions of 63-106, 106-150, and 150-300 μm , and three different dosages of dodecylamine, as the collector, were tested. According to the results obtained, the particle size fraction of 106-150 μm had the maximum bubble loading for bubble diameter of 1.8 mm, while the particle size of 63-106 μm had the maximum bubble loading for bubble diameter of 0.8 mm. It was also shown that increasing the bubble diameter from 0.8 to 1.8 mm increased the bubble loading in all the particle size fractions and collector dosages. However, the mass loading of air bubbles was strongly related to the collector dosage (contact angle), especially for coarse particles. The amount of collector dosage had an upper limit due to the clustering event, which significantly affected the bubble loading. The clustering was found to be more important in the presence of small particles due to a higher number of particles attached to the bubble surface. It was shown that such interactions of variables of true flotation could reasonably be monitored by the bubble loading measurement.

Keyword: *Column Flotation, Bubble Loading, Bubble Size, Particle Size, Collector Dosage.*

1. Introduction

Flotation is a physico-chemical separation process, which is widely used to separate the desired group of particles from the bulk of undesired materials [1]. The successful operation of a flotation process depends upon some particular variables such as the bubble and particle sizes and the reagent concentration [2]. The bubble and particle sizes are physical variables that are intimately linked to the bubble-particle collision [3]. The collector dosage, as a chemical variable, dictates the surface characteristics of solid particles, and thereupon influences the attachment and detachment sub-processes [2, 4]. So far, the effects of bubble size, particle size, and reagent dosage on the flotation performance of different minerals have been studied by many

researchers [2, 5-18], among which Rahman et al. [2] have used a unique device to investigate the flotation behavior of different particle sizes and their response to changes in the other operating variables, and have concluded that the presence of fine particles is imperative for enhancement of the flotation of coarse particles. Crawford and Ralston [9] have investigated the flotation behavior of quartz particles over the particle diameters ranged from 15 to 125 μm using a known bubble size, and have concluded that for a specific particle size, there is a contact angle below which the mineral will not float. Lee et al. [11] have shown that the flotation rate constant and the collection efficiency are greatly affected by the changes in the bubble size and particle size in a flotation

column. Santana et al. [15] have studied the flotation performance of apatite particles as a function of particle size and reagent dosage in a flotation column, showing that there is an optimum particle size with regard to the reagent dosage in order to achieve a satisfactory flotation performance. Muganda et al. [17] have investigated the influence of particle size and contact angle on the flotation of chalcopyrite, showing that the flotation rate increases rapidly with an increase in the contact angle for particles in the intermediate size fractions, and the critical contact angle for the floatability of mineral particles varies with the particle size fraction. Hassanzadeh et al. [18] have concluded that the collision efficiency of fine particles is improved with bubbles of finer sizes, and in a known particle size range, the collision efficiency decreases with increase in the bubble velocity. However, the effects of bubble and particle sizes and reagent concentration on a true flotation (no entrainment and no froth zone effects) have not been addressed before, including the relationship between these variables and the mass loaded on air bubbles (specifically, in column flotation). Bubble loading is a macroscopic measure that includes the micro sub-processes of true flotation [19]. The present work aimed to study the interactional effects of the physical and chemical operating variables (bubble and particle sizes and collector dosage) on bubble loading under the steady state condition in a continuous column flotation.

2. Materials and methods

The bubble loading measurements were performed under a continuous steady-state condition using the methodology presented by Hemmati Chegeni and co-workers [19] including a laboratory column (5.4 cm diam. × 116 cm height) with a laminar flow regime and least mixing, a needle sparging system to produce a narrow bubble size distribution (BSD), and a bubble sampler with an internal diameter of 2 cm and a height of 72 cm. A schematic diagram of the experimental set-up is shown in Figure 1. The details of the apparatus specifications and experimental run procedure are available in the literature [19].

Pure quartz (99.64%, 2.65 g/cm³) in three size fractions of 63-106, 106-150, and 150-300 μm was used to prepare the flotation pulp. The XRF

analysis of the mineral is presented in Table 1. In the present work, the mineral samples were washed by a solution composed of H₂SO₄ (2.5% by volume) and NaOH (2.5% by weight), and then rinsed with deionized water to ensure that the particles were free of any contamination, and their surface was hydrophilic. The cleaned mineral samples were then left to dry in a clean room environment. Dodecylammonium chloride (0.5 g/L of dodecylamine solution in HCl at pH = 3) and A65 (polypropylene glycol) were the collector and the frother reagents, respectively. Sodium hydroxide was used to adjust the pH value. It is worthy of notice that dodecylamine has a soap-like solid form at room temperature so it cannot be conditioned with the flotation pulp in its stable form. Therefore, as an alternative, it should be dissolved in a fairly acidic solution to be transformed into its liquid form in order to be used efficiently in the conditioning process. The three collector dosages of 50, 100, and 150 g/Mg and the two bubble sizes of 0.8 and 1.8 mm with a low standard deviation of BSD were tested. BSD was analyzed using the codes developed in the image processing toolbox of MATLAB[®]. The images were acquired by a digital camera (Dino-Lite Digital Microscope AM-7013M) using a HUT bubble analyzer, as shown in Figure 2. The contact angles for different collector dosages were determined using the Washburn technique [20] in accordance with [21]. Similar to all the previous studies on bubble loading, except for the single bubble investigations, the measured bubble loading in this work indicates the “mean” mass of solid particles attached per unit surface of air, as the captured bubbles may be loaded with different numbers of particles. Besides, due to the design of the experimental set-up, no entrainment of unattached particles was possible in flotation runs (as explained by [19]). The test procedure and experimental condition were determined through conducting several rudimentary tests with regard to the procedures and conditions determined by the other researchers, and finally, an optimum experimental procedure was determined. A summary of the experimental conditions is presented in Table 2. A multi-level categoric factorial experimental design was executed requiring 18 experiments. Replicate experiments were also performed in order to evaluate the reproducibility of the results.

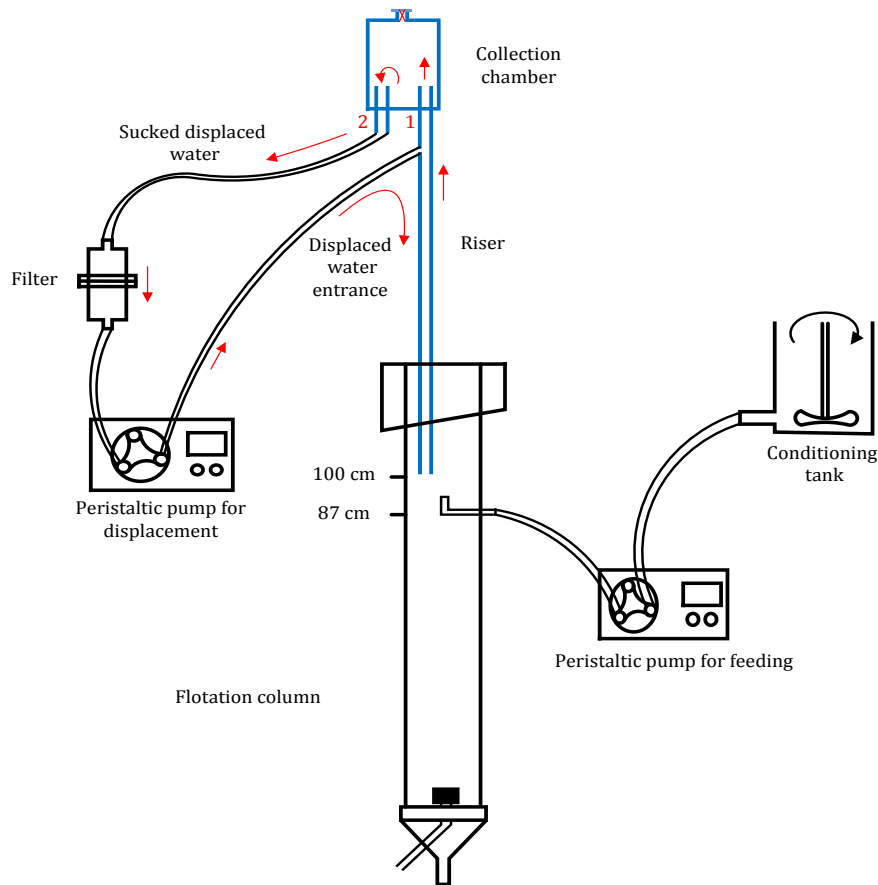


Figure 1. Schematic diagram of experimental set-up used for bubble loading measurements [19].

Table 1. Results of XRF analysis.

%	Composition	%	Composition
0.005	P ₂ O ₅	99.64	SiO ₂
0.011	TiO ₂	0.05	Al ₂ O ₃
0.001	MnO	0.31	Fe ₂ O ₃
0.03	L.O.I	0.06	CaO
24	Ba (ppm)	0.01	Na ₂ O
15	Cl (ppm)	0.01	MgO
7	S (ppm)	0.01	K ₂ O

Table 2. Experimental conditions for bubble loading measurement.

Feeding rate (cm ³ /min)	847	Feed solid weight (g)	300
Aeration rate (cm ³ /min)	300	Feed solid content (%)	10
Sampling time (s)	120	Pulp conditioning time (min)	10
Frother dosage for small bubbles (ppm)	45	Impeller speed in pulp conditioning (rpm)	250
Frother dosage for large bubbles (ppm)	30	Bubble sizes (mm)	0.8 and 1.8
pH	7	Collector Dosages (g/Mg)	50, 100 and 150
Time to achieve steady state condition (s)	40	Dodecylamine (g/L)	0.5
Frother conditioning time (min)	10		

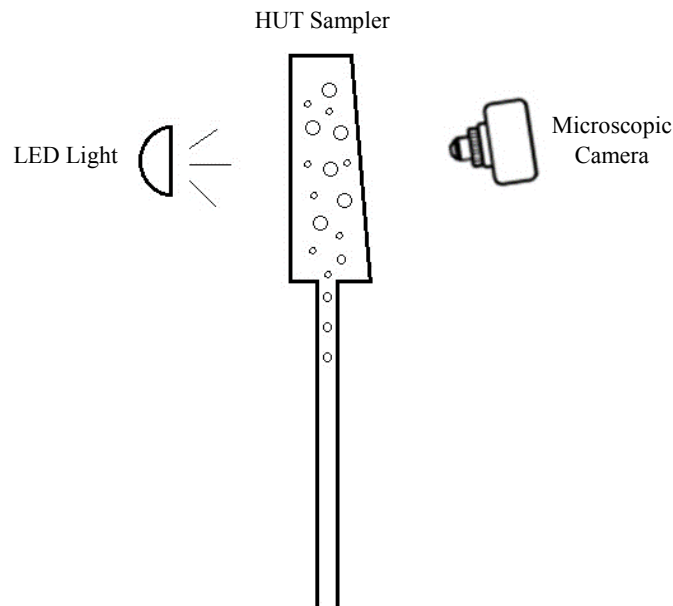


Figure 2. Schematic representation of image acquisition apparatus for BSD analysis.

2.1. Bubble loading measurement

In order to measure the bubble loading, first of all, the aeration system (sparger) at the bottom of the column was opened, and then the column was filled with the frother-water mixture (prepared earlier) to prevent bubble coalescence within the column, and also to get the column ready for the next steps. The nozzle at the bottom of the riser tube of the sampler was closed with a bung, and then the sampler was inserted into the flotation cell so that the nozzle was located at the target height (100 cm) in the collection zone, where the sampler was fixed. Later on, the sampler was also filled with the frother-water mixture to prevent bubbles from coalescing during sampling. Afterwards, the upper orifice of the sampler was closed with a bung as well. Outside the column, the pulp was conditioned with the cationic collector for 10 min and then was fed into the column with a feeding rate of 0.847 L/min for 60 s until the column was completely filled with the slurry. Then the bung was removed from the bottom of the riser to let the floated bubbles (loaded and unloaded) enter the collection chamber through the riser tube for about 120 s. Upon reaching the collection chamber, the bubbles burst at the liquid/gas interface in the chamber, and the particles were detached. The detached particles then settled to the lower part of the chamber, while the air volume was accumulated in its upper part. Displaced water-frother solution, equivalent to the total volume of the accumulated bubbles, exited the chamber through the outlet #2 (see Figure 1) based on the positive displacement principle with the help of a

peristaltic pump, and then passed through the filter to capture any suspended solid particles, preventing them from entering the flotation cell. The displaced water was then recycled to the riser tube through the displaced water entrance, as shown in Figure 1. The counter-current flow of the displaced water within the riser tube helped prevent any possible entrained particles to enter the collection chamber. The bias velocity of the displaced water in the riser tube was adjusted via pump speed, where a bias velocity of less than or equal to the superficial gas velocity was maintained in order to prevent loaded particles being detached from aggregates in the riser tube as well as allowing the entrained particles to return down to the cell. At the end of the experiment, the tailing outlet (discharge valve) of the column was opened immediately to drain all the pulp out of the column, where, at the same time, the suction rate of the peristaltic pump was increased until the remaining water in the collection chamber was completely drained and passed through the filter to ensure that no sample loss occurred. The sampling time was recorded along with the volume of water displaced (volume of air accumulated), and the mass of particles trapped in the device as well as in the filter. The collected particles were then dried and weighed, and then using the calculation procedure presented by [19], bubble loading was quantified.

3. Results and discussion

3.1. Bubble loading results

Results of bubble loading measurements are shown in Table 3.

Table 3. Bubble loading results for different operating conditions.

Operating variables			Bubble loading results (mg/mm ²)			
Bubble size (mm)	Collector dosage (g/Mg)	Particle size (μm)	Mean	Min.	Max.	Standard deviation
0.8	50	+63-106	0.0114714	0.010065	0.013456	0.0013996
		+106-150	0.0052511	0.0049756	0.0056245	0.0003063
		+150-300	0.0002748	0.000249	0.000304	2.31E-05
	100	+63-106	0.019464	0.01856	0.02045	0.0008619
		+106-150	0.0146081	0.0138545	0.0156424	0.0008213
		+150-300	0.0023628	0.002174	0.002546	0.0001582
	150	+63-106	0.0142325	0.012987	0.015356	0.0010945
		+106-150	0.0133925	0.0118987	0.0148978	0.0012189
		+150-300	0.0070661	0.006958	0.007245	0.0001579
1.8	50	+63-106	0.0152045	0.014326	0.015745	0.0006893
		+106-150	0.0175131	0.015896	0.018785	0.0011659
		+150-300	0.0011056	0.001011	0.001232	0.0000932
	100	+63-106	0.0303745	0.028894	0.031526	0.0012235
		+106-150	0.0323079	0.030561	0.033785	0.0014257
		+150-300	0.0064669	0.0060452	0.0068515	0.0003493
	150	+63-106	0.0276084	0.026789	0.028897	0.0009194
		+106-150	0.0304372	0.029456	0.031546	0.0011068
		+150-300	0.0205056	0.019234	0.021789	0.0010541

3.2. Particle size effect

Effect of different particle size fractions on the bubble loading was investigated in the presence of different bubble sizes and collector dosages, and the results obtained were depicted in Figure 3. According to Figure 3-a, for the bubble size of 1.8 mm, an increase in the particle size from 63-106 μm to 106-150 μm gave a meager rise to bubble loading, while for a 150-300 μm particle size, the bubble loading dropped remarkably in any dosage of the collector. This could be attributed to the fact that in the presence of coarse particles, the detachment probability of solid particles from bubble surfaces increases, specifically in turbulent zones [22]. In addition, 106-150 μm was observed as the optimum particle size range for bubble loading when large bubbles were used. The poor bubble loading of small particles in the presence of large bubbles is mainly due to their low collision efficiencies due to their lower mass and inertial force, which can be improved with bubbles of small sizes [18, 23]. For a bubble size of 0.8 mm, however, 63-106 μm was observed as the optimum size range, where bubble loading was maximum, as shown in Figure 3-b. However, in the same condition, the maximum bubble loading for the coarse bubbles was higher than the maximum bubble loading for the small bubbles.

3.3. Bubble size effect

According to Figure 4, bubble loading increase with increase in the bubble size from 0.8 mm to 1.8 mm. This is because in the presence of large

bubbles, the buoyancy force and the mass loading power of air bubbles are improved [12]. In addition, with increase in the bubble size, the bubble-particle attachment efficiency increases as well [12]. Moreover, in the same particle size, the active surface of large bubbles, which is feasible for particle attachment, is greater than that of small bubbles [24].

3.4. Collector dosage effect

In order to investigate the effect of collector dosage (contact angle) on the mass loading on air bubbles, three different collector dosages (i.e. 50, 100, and 150 g/Mg) were tested. According to Figure 5, for the particle sizes of 63-106 μm and 106-150 μm, the bubble loading increased with increase in the collector dosage from 50 to 100 g/Mg, where the optimum collector dosage was 100 g/Mg for both 0.8 and 1.8 mm of bubble size. However, under the same conditions, increasing the collector dosage up to 150 g/Mg led to a drop in the bubble loading. This is because of the bubble-clustering phenomenon, which, in this work, happened when the collector concentration within the pulp increased up to 150 g/Mg. The bubble-clustering phenomenon happens when the collector concentration within a pulp increases up to a certain point, and extremely hydrophobic particles attach to two or more small-size bubbles (particle bridging) [25, 26]. As a result, in such a circumstance, the available specific surface of air bubbles for particle collection decreased

remarkably, and this negatively affected the bubble loading. For the particle size of 150-300 μm , however, it was observed that bubble loading increased with increase in the collector dosage from 50 to 150 g/Mg. This implies that the cluster formation does not take place in the presence of this particle size when the collector concentration increases up to 150 g/Mg. According to the results obtained, this might be because in the flotation of coarse particles (in this case, 150-300 μm), specifically when large-size bubbles are used, there are only a countable number of solid

particles attached to the surface of an individual air bubble, and such a number of particles is not enough to build particle bridges between two or more bubbles to form clusters. In addition to the above-mentioned interpretations, it is also shown in Figure 5 that small-size bubbles are more prone to the clustering event, as compared to the large-size bubbles in a similar condition. Figure 6 presents a visual evidence of the formation of bubble clusters in the present work. The measured contact angles for different collector dosages are presented in Table 4.

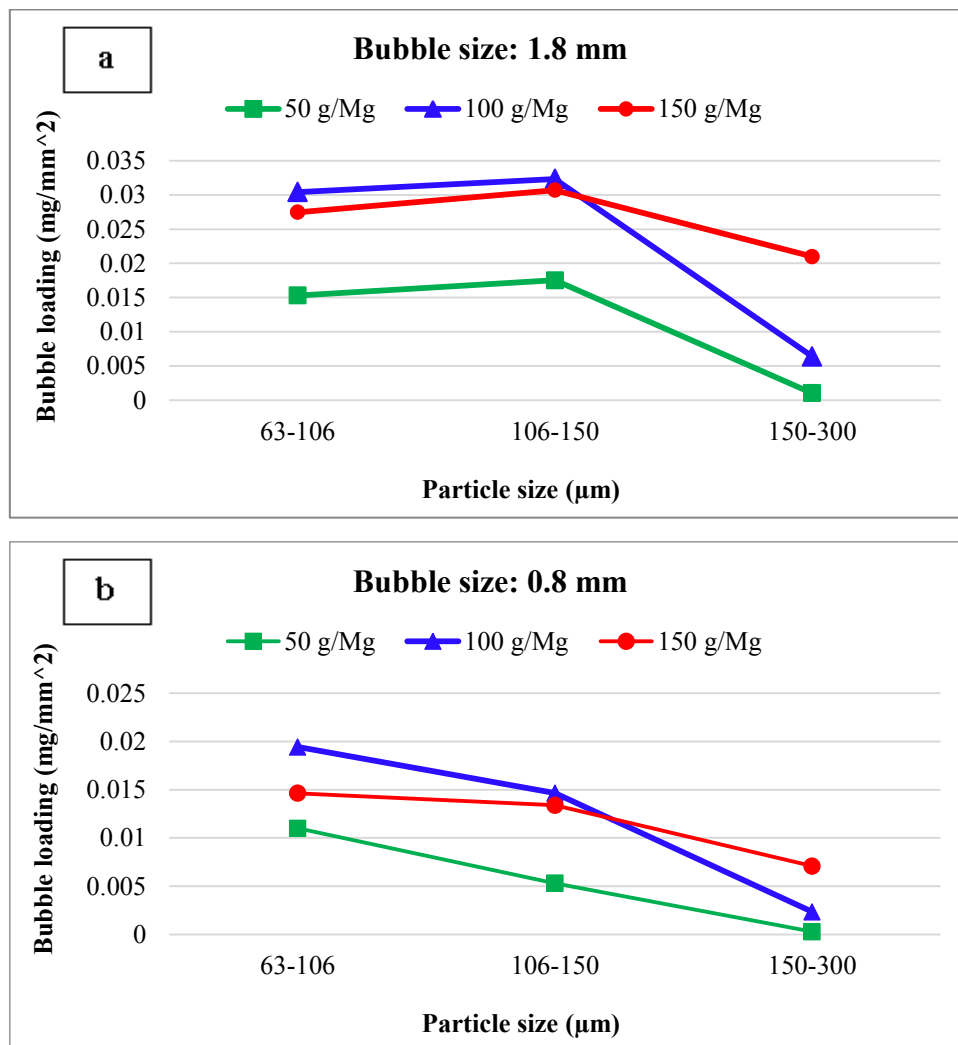


Figure 3. Effects of particle size on bubble loading in different bubble sizes.

Table 4. Contact angles for different collector dosages.

Collector (g/Mg)	Collector (mol/L)	Contact angle
50	30×10^{-6}	27°
100	59.9×10^{-6}	32°
150	89.9×10^{-6}	38°

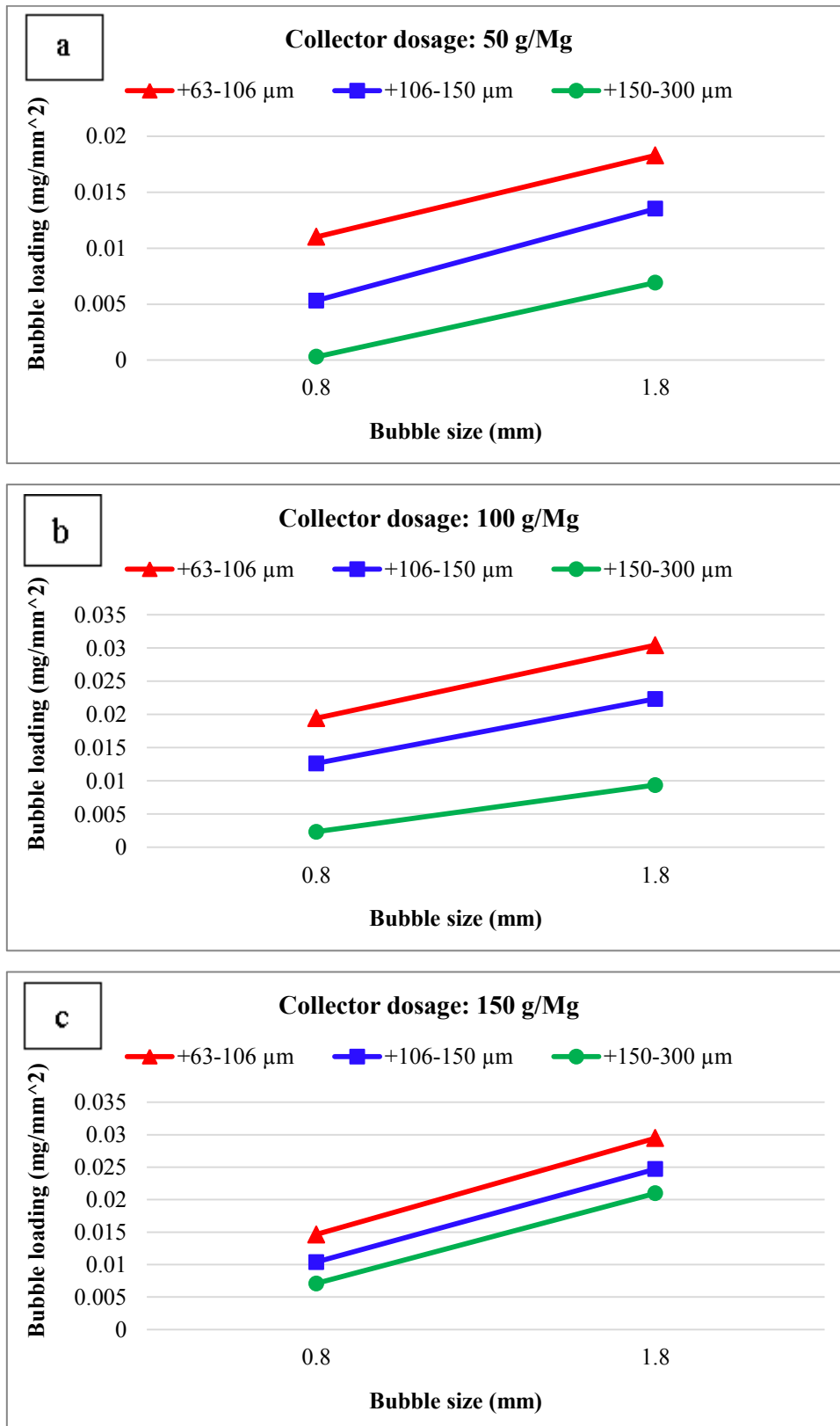


Figure 4. Effects of bubble size on bubble loading in different collector dosages.

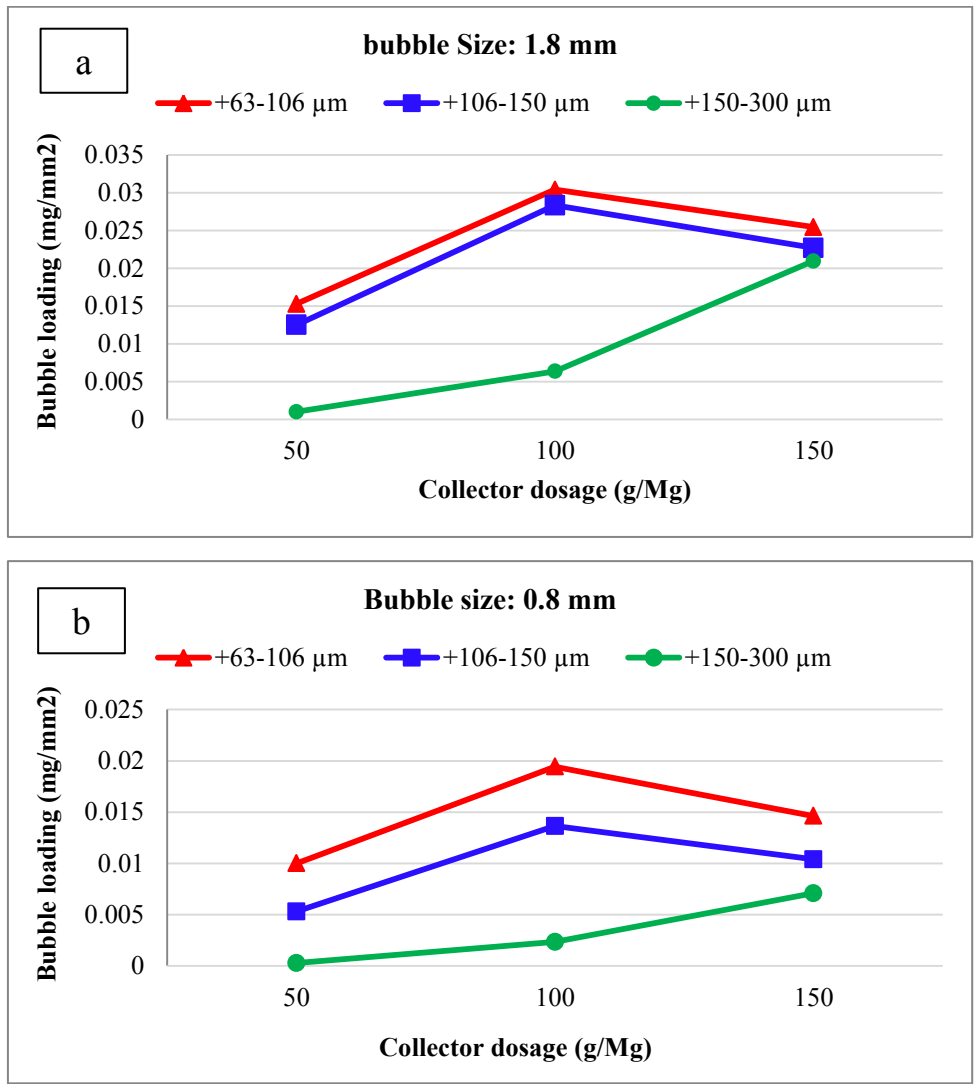


Figure 5. Effects of collector dosage on bubble loading in different particle and bubble sizes.

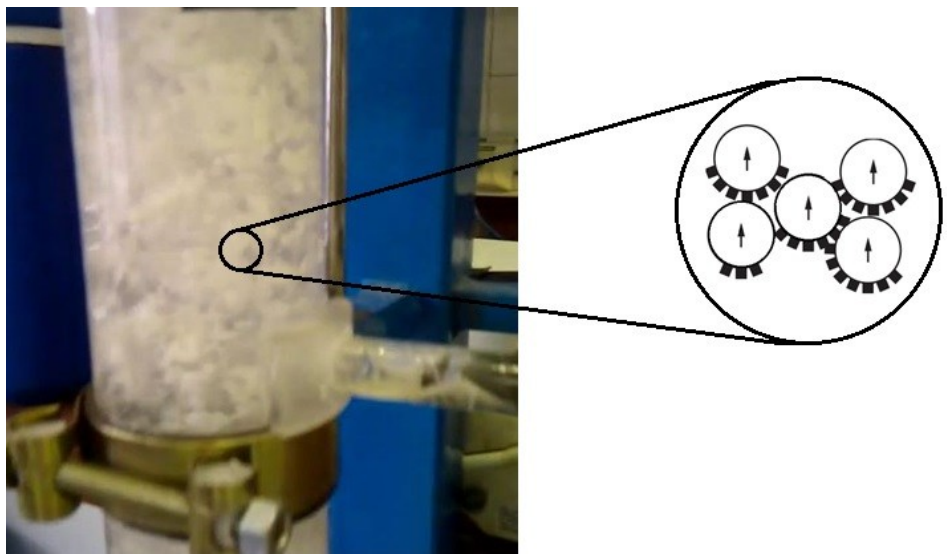


Figure 6. Bubble cluster formation within pulp zone.

4. Conclusions

Bubble loading measurements were used in this work to investigate the interactional effects of the main physical and chemical variables of the true flotation process in column flotation, as these measurements are not affected by the entrainment or froth phase. The results obtained show that for a given particle density, the optimum particle size for maximum bubble loading is related to the bubble size. For quartz (2.65 g/cm^3), among the three tested size fractions, 106–150 μm showed the maximum bubble loading for a 1.8 mm bubble diameter under the discussed operational conditions. This optimum size reduced to 63–106 μm for a 0.8 mm bubble size.

The bubble loading increased with increase in the bubble size, even though the increasing rate is strongly related to the particle contact angle or collector dosage. The effect of contact angle is more significant for coarse particles. Increasing the contact angle is limited by the maximum amount of collector usage due to the clustering event. This limited amount of collector is related to the number of particles attached on the bubble surface. In the presence of small particles, clustering occurs with a rather lower amount of collector compared to coarse particles. Such interactions between the main physical and chemical variables of true flotation measured by bubble loading indicate the lack of a comprehensive model of the bubble loading process.

References

[1]. Wills, B.A. and Finch, J.A. (2016). Chapter 12-Froth Flotation Wills' Mineral Processing Technology (Eighth Edition) (pp. 265-380). Boston: Butterworth-Heinemann.

[2]. Rahman, R.M., Ata, S. and Jameson, G.J. (2012). The effect of flotation variables on the recovery of different particle size fractions in the froth and the pulp. *International Journal of Mineral Processing*. 106: 70-77.

[3]. Ahmed, N. and Jameson, G.J. (1985). The effect of bubble size on the rate of flotation of fine particles. *International Journal of Mineral Processing*. 14 (3): 195-215.

[4]. Somasundaran, P. and Wang, D. (2006). *Solution chemistry: minerals and reagents* (Vol. 17). Elsevier.

[5]. Bartlett, D.R. and Mular, A.L. (1974). Dependence of flotation rate on particle size and fractional mineral content. *International Journal of Mineral Processing*. 1 (3): 277-286.

[6]. Mehrotra, S.P. and Kapur, P.C. (1975). The effects of particle size and feed rate on the flotation rate distribution in a continuous cell. *International Journal of Mineral Processing*. 2 (1): 15-28.

[7]. Trahar, W.J. (1976). The selective flotation of galena from sphalerite with special reference to the effects of particle size. *International Journal of Mineral Processing*. 3 (2): 151-166.

[8]. Trahar, W.J. (1981). A rational interpretation of the role of particle size in flotation. *International Journal of Mineral Processing*. 8 (4): 289-327.

[9]. Crawford, R. and Ralston, J. (1988). The influence of particle size and contact angle in mineral flotation. *International Journal of Mineral Processing*. 23 (1-2): 1-24.

[10]. Gopalratnam, V.C., Bennett, G.F. and Peters, R.W. (1992). Effect of collector dosage on metal removal by precipitation/flotation. *Journal of Environmental Engineering*. 118 (6): 923-948.

[11]. Lee, J.E. and Lee, J.K. (2002). Effect of microbubbles and particle size on the particle collection in the column flotation. *Korean Journal of Chemical Engineering*. 19 (4): 703-710.

[12]. Tao, D. (2005). Role of bubble size in flotation of coarse and fine particles- a review. *Separation Science and Technology*. 39 (4): 741-760.

[13]. Bravo, S.V.C., Torem, M.L., Monte, M.B.M., Dutra, A.J.B. and Tondo, L.A. (2005). The influence of particle size and collector on the flotation of a very low grade auriferous ore. *Minerals Engineering*. 18 (4): 459-461.

[14]. Uçurum, M. and Bayat, O. (2007). Effects of operating variables on modified flotation parameters in the mineral separation. *Separation and Purification Technology*. 55 (2): 173-181.

[15]. Santana, R.C., Farnese, A.C., Fortes, M.C., Ataíde, C.H. and Barrozo, M.A. (2008). Influence of particle size and reagent dosage on the performance of apatite flotation. *Separation and Purification Technology*. 64 (1): 8-15.

[16]. Santana, R.C., Duarte, C.R., Ataíde, C.H. and Barrozo, M.A.S. (2011). Flotation selectivity of phosphate ore: Effects of particle size and reagent concentration. *Separation Science and Technology*. 46 (9): 1511-1518.

[17]. Muganda, S., Zanin, M. and Grano, S.R. (2011). Influence of particle size and contact angle on the flotation of chalcopyrite in a laboratory batch flotation cell. *International Journal of Mineral Processing*. 98 (3): 150-162.

[18]. Hassanzadeh, A., Hassas, B.V., Kouachi, S., Brabcova, Z. and Celik, M.S. (2016). Effect of bubble size and velocity on collision efficiency in chalcopyrite

flotation. *Colloids and Surfaces A: Physicochemical and Engineering Aspects*. 498: 258-267.

[19]. Hemmati Chegeni, M., Abdollahy, M. and Khalesi, M.R. (2016). Bubble loading measurement in a continuous flotation column. *Minerals Engineering*. 85: 49-54.

[20]. Washburn, E.W. (1921). The dynamics of capillary flow. *Physical review*. 17 (3): 273.

[21]. Chau, T.T. (2009). A review of techniques for measurement of contact angles and their applicability on mineral surfaces. *Minerals Engineering*. 22 (3): 213-219.

[22]. Finch, J.A. and Dobby, G.S. (1990). *Column Flotation*. Pergamon Oxford.

[23]. Schulze, H.J., Radoev, B., Geidel, T., Stechemesser, H. and Töpfer, E. (1989). Investigations of the collision process between particles and gas bubbles in flotation- A theoretical analysis. *International Journal of Mineral Processing*. 27 (3-4): 263-278.

[24]. Ralston, J., Fornasiero, D. and Hayes, R. (1999). Bubble- particle attachment and detachment in flotation. *International Journal of Mineral Processing*. 56 (1): 133-164.

[25]. Schulze, H.J. (1983). *Physicochemical elementary processes in flotation*. Elsevier Science Publishers. 348 P.

[26]. Ata, S. and Jameson, G.J. (2005). The formation of bubble clusters in flotation cells. *International Journal of Mineral Processing*. 76 (1): 123-139.

اثرات متقابل اندازه حباب، اندازه ذره و مقدار کلکتور بر بارگیری حباب در فلوتاسیون ستونی

امیر اسکانلو^۱، محمدرضا خالصی^{۱*}، محمود عبدالهی^۱ و محسن همتی چگنی^۲

۱- بخش مهندسی معدن، دانشکده فنی مهندسی، دانشگاه تربیت مدرس، ایران

۲- بخش مهندسی معدن، دانشگاه صنعتی اراک، ایران

ارسال ۲۰۱۷/۵/۲۹، پذیرش ۲۰۱۷/۷/۱۶

* نویسنده مسئول مکاتبات: mrkhalesi@modares.ac.ir

چکیده:

موفقیت عملیات فلوتاسیون به برآیند موفق اثرات متقابل میان متغیرهای فیزیکی و شیمیایی وابسته است. در این تحقیق، اثرات فاکتورهای اندازه ذره، اندازه حباب و مقدار کلکتور بر بارگیری حباب در یک ستون فلوتاسیون با کارکرد پیوسته مورد بررسی قرار گرفت؛ به عبارت دیگر، این تحقیق به ارزیابی پاسخ فرآیند فلوتاسیون صحیح به تغییرات ممکن در متغیرهای کاربردی در فلوتاسیون ستونی پرداخته است. در این خصوص، دو اندازه حباب $0/8$ و $1/8$ mm، سه اندازه ذره $63-106$ ، $106-150$ و $150-300$ μm و سه مقدار مختلف از کلکتور دودسیل آمین مورد آزمایش قرار گرفتند. بر اساس نتایج حاصل، مقدار بیشینه بارگیری حباب در اندازه ذره $106-150$ μm در حضور اندازه حباب $1/8$ mm مشاهده شد، در حالی که این مقدار بیشینه در اندازه ذره $63-106$ μm در حضور اندازه حباب $0/8$ mm به دست آمد. همچنین، افزایش اندازه حباب از $0/8$ تا $1/8$ mm موجب افزایش بارگیری حباب در تمامی اندازه ذرات و مقادیر کلکتور شد. با این وجود، بارگیری ذرات جامد بر روی حباب‌های هوا وابستگی شدیدی به مقدار کلکتور مصرفی (زاویه تماس) از خود نشان داد، به خصوص برای ذرات درشت. مقدار کلکتور مصرفی در اثر وقوع پدیده خوشه‌ای شدن حباب‌ها، یک حد بالای معینی را از خود نشان داد که بالاتر از آن بارگیری حباب به شدت تحت تأثیر منفی این پدیده قرار گرفت. مشاهده شد که احتمال وقوع پدیده خوشه‌ای شدن حباب‌ها در حضور ذرات با اندازه نسبی کوچک بیشتر است زیرا در این صورت ذرات جامد با تعداد بیشتری امکان چسبیدن بر سطح حباب را دارند. در این تحقیق نشان داده شد که این قبیل اثرات متقابل میان متغیرهای فلوتاسیون صحیح را می‌توان با اندازه‌گیری بارگیری حباب مورد پایش قرار داد.

کلمات کلیدی: فلوتاسیون ستونی، بارگیری حباب، اندازه حباب، اندازه ذره، مقدار کلکتور.